Published in final edited form as:
Mitochondrion. 2010 June ; 10(4): 342–349. doi:10.1016/j.mito.2010.02.004.

MnSOD activity protects mitochondrial morphology of quiescent fibroblasts from age associated abnormalities

Ehab H. Sarsour, **Monali Goswami**, **Amanda L. Kalen**, and **Prabhat C. Goswami**
Free Radical and Radiation Biology Program, Department of Radiation Oncology, University of Iowa, Iowa City, USA

Abstract

Previously, we have shown manganese superoxide dismutase (MnSOD) activity protects quiescent human normal skin fibroblasts (NHFs) from age associated loss in proliferative capacity. The loss in proliferative capacity of aged *vs*. young quiescent cells is often characterized as the chronological life span, which is clearly distinct from replicative senescence. We investigate the hypothesis that MnSOD activity protects the mitochondrial morphology from age associated damage and preserves the chronological life span of quiescent fibroblasts. Aged quiescent NHFs exhibited abnormalities in mitochondrial morphology including abnormal cristae formation and increased number of vacuoles. These results correlate with the levels of cellular reactive oxygen species (ROS) and mitochondrial morphology in MnSOD homozygous and heterozygous knockout mouse embryonic fibroblasts. The abnormalities in mitochondrial morphology in aged quiescent NHFs cultured in presence of 21% oxygen concentration were more severe than NHFs cultured in 4% oxygen environment. The alteration in mitochondrial morphology was associated with a significant increase in cell population doubling: 54 h in 21% compared to 44 h in 4% oxygen environment. Overexpression of MnSOD decreased ROS levels, and preserved mitochondrial morphology in aged quiescent NHFs. These results demonstrate that MnSOD activity protects mitochondrial morphology and preserves the proliferative capacities of quiescent NHFs from age associated loss.

Keywords

MnSOD; mitochondria; quiescent growth; ROS; Aging; Chronological life span

1. Introduction

Aging is a complex process both at the organism and cellular levels. The classical observation of Hayflick relates to a finite number of cell divisions in normal cells prior to irreversible growth arrest, “Hayflick limit” (Hayflick and Moorhead 1961). Subsequent research characterized this phenomenon of cellular aging as the telomere shortening theory of aging, also known as replicative senescence (Campisi 2000; Smith and Pereira-Smith 1996). While the majority of research is focused on understanding the mechanisms regulating replicative

Corresponding author: Ehab H. Sarsour, PhD, Free Radical & Radiation Biology Program, Department of Radiation Oncology, The University of Iowa, B180 Medical Laboratories, Iowa City, Iowa-52242, Phone: (319) 335-8025, Fax: (319) 335-8039, ehab-sarsour@uiowa.edu.

senescence, an earlier study reports a replication independent phenomenon of cellular aging known as “chronological life span”(Harris et al. 2003). The chronological life span is defined as the age associated loss in the proliferative capacity of quiescent cells. Cellular quiescence is a reversible growth state that is highly essential for cell and tissue renewal, and to avoid aberrant proliferation. In general, a majority of cells *in vivo* reside in a quiescent growth state, e.g. adult stem cells, progenitor cells of the bone marrow, and cells in the intestines. Therefore, a better understanding of the mechanisms regulating the proliferative capacity of quiescent cells, chronological life span, is warranted.

A regulatory role of reactive oxygen species (ROS) in aging, the “free radical theory of aging”, was originally suggested by D. Harman in 1956 (Harman 1956). The free radical theory of aging is also known as the error theory of aging that describes age associated accumulation of damage to cellular macromolecules and organelles (Finkel and Holbrook 2000). ROS are generated both from exogenous and endogenous sources. Mitochondrial metabolism and other oxygen utilizing enzymes are the major endogenous sources of ROS. Oxygen is the terminal electron acceptor in the respiratory chain of mitochondria during energy production. While this process is highly efficient, it was estimated earlier that approximately 1–2 percent of oxygen is converted to ROS (Chance 1977; Chance et al. 1979). However, more recent studies estimated that approximately 0.2–0.8 percent oxygen is converted to ROS in physiological conditions (Balaban et al. 2005; St-Pierre et al. 2002; Staniek and Nohl 2000). This is still a significant amount of ROS accumulation considering the cumulative nature of oxidative damage during cellular and organism aging. Because mitochondria are the major source of ROS (superoxide and hydrogen peroxide) production, a higher threshold of ROS can damage mitochondrial morphology.

Eukaryotic cells evolved with elaborate defense mechanisms to protect themselves from ROS induced oxidative damage. This defense system includes the cellular antioxidant enzymes and small molecular weight antioxidants. Superoxide dismutase converts superoxide to hydrogen peroxide, which is neutralized by catalase and glutathione peroxidase. MnSOD is a nuclear encoded and mitochondrial matrix localized homotetrameric enzyme that removes mitochondrially generated superoxide (Borgstahl et al. 1992; Boveris 1977). CuZnSOD is present in the cytoplasm, nucleus, and mitochondrial inner membrane space, while EcSOD is present in the plasma membrane and extracellular space (Finch 2003). An increase in ROS levels and the subsequent changes in mitochondrial morphology of aged quiescent cells could result from an increase in the production of ROS or a decrease in ROS removal probably due to changes in cellular antioxidant capacity. Consistent with this notion, MnSOD knockout mice showed significant damage in the activities of mitochondrial aconitase, complex I, and succinate dehydrogenase (Li et al. 1995). Furthermore, these mice exhibited many of the symptoms seen in children with genetic defects of the respiratory chain, e.g. lactic acidaemia, cardiomyopathy, and the degeneration of the basal ganglia (Li et al. 1995). Overexpression of MnSOD has been shown to extend Drosophila lifespan (Orr and Sohal 1994). Likewise, the SOD and catalase mimetic, Eukarion (EUK-8, 134, and 189), increased the lifespan of MnSOD homozygous knockout mice approximately three-fold (Melov et al. 2001; Melov et al. 1998). However, a recent study showed that overexpression of MnSOD, CuZnSOD, and catalase, individually or in combination, did not extend the life span of C57BL/6J mice (Perez et al. 2009). These differences in results could be due to the disparities in the concentrations (threshold) of ROS, pulse duration (flux), sub-cellular localization, species, and cell and tissue types. Furthermore, because chronological life span relates more towards the age-dependent decline in cell and tissue renewal, additional studies are needed to determine whether an efficient antioxidant system is better poised to counter oxidative stress and wound healing, and maintain an overall quality of life during aging.

We have shown previously overexpression of MnSOD protects quiescent normal human skin fibroblasts from age associated loss in proliferative capacity (Sarsour et al. 2005). This protection is associated with an inhibition in age associated accumulation of p16 cyclin dependent kinase inhibitor protein levels. Results from this study show that MnSOD activity protects quiescent normal human skin fibroblasts (NHFs) from age associated accumulation of ROS and abnormalities in mitochondrial morphology, and preserves the proliferative capacity of quiescent NHFs.

2. Materials and methods

2.1 Cell culture

Human normal skin fibroblasts (AG01522) from a 3 day old male of non-fetal origin were obtained from Coriell Cell Repositories. MnSOD knockout mouse embryonic fibroblasts (MEFs) (MnSOD −/−), heterozygous (MnSOD +/−), and wild type (MnSOD +/+) cells were generously provided by Dr. T. T Huang (Stanford University, CA, USA). Cells were obtained from Sod2 mutant mice, which were originally produced in the CD1 strain of mice. Heterozygous (Sod2 +/−) mice were backcrossed to C57BL/6J and DBA/2J mice for 17 and 12 generations, respectively. The cells used in this study were from the first generation offspring of congenic heterozygous C57BL/6J and DBA/2J mice, designated as B6D2F1 Sod2 mutant (Sod2 −/−), (Sod2 +/−), and (Sod2 +/+) mice (Asikainen et al. 2002; Li et al. 1995). Cells were cultured in Dulbecco's modified Eagle's medium containing 10% fetal bovine serum and antibiotics in incubators with controlled temperature of 37°C, 5% CO_2, and 95% humidity. MnSOD genotype MEFs were cultured in 4% O_2 environment. All experiments with human normal skin fibroblasts (NHFs) were performed using passage 7–8, and passage 3–4 was used for the mouse fibroblasts.

Cell numbers were counted using a Coulter Counter (Beckman-Coulter, USA). Cell population doubling times were calculated using the following equation: Td=0.693t/ln(Nt/N0) where t is time in days, and Nt and N0 represent cell numbers at time t and the initial time, respectively.

2.2 Adenoviral mediated overexpression of MnSOD

Replication-deficient adenoviruses containing cytomegalovirus promoter driven wild type human MnSOD cDNA (AdMnSOD) were obtained from The University of Iowa DNA-Vector Core Facility. MnSOD cDNA was inserted into the E1 region of an E1/partial E3-deleted replication-deficient adenoviral vector. A non-modified vector (AdBgl II) was used as control for adenoviral infections (Davidson et al. 1993; Liu et al. 1997). Fibroblasts were infected with 10–30 multiplicity of infection (MOI) in serum free media for 24 h followed by addition of regular medium containing 10% serum (Sarsour et al. 2005; Sarsour et al. 2008). MnSOD overexpression was verified by performing immunoblotting assay, and activities measured using gel electrophoresis based assay (Sarsour et al. 2005; Sarsour et al. 2008).

2.3 Transmission electron microscopy

Cells were collected by scraping, washed with cold PBS, and fixed with 2.5% glutaraldehyde in 0.1 M Na-cacodylate buffer. Fixed cells were incubated with 1% Osmium tetroxide for 2 h and processed for embedding; incubation with distilled water for 1 min, 20 min in 2.5% uranyl acetate, 15 min in 50% ethanol, 15 min in 70% ethanol, 30 min in 95% ethanol, 2×30 min in 100% ethanol, 1 h in ethanol and Epon (2:1), 1 h in ethanol and Epon (1:2), and overnight in 100% Epon in a 60°C oven. Ultra thin sections, 70 nm, were placed on a 200 mesh copper grids, and stained with 5% uranyl acetate and lead citrate. Samples were visualized using JEOL 1230 transmission electron microscopy. All microscopy measurements were performed using The University of Iowa Central Microscopy Research Core Facility.

2.4 Immunoblotting assay

Total cellular protein extracts were prepared by sonication using a Vibra Cell Sonicator with cup attachment (Sonics and Materials Inc., Newtown, CT, USA), and protein concentrations were determined using Bradford protein assay (Bio-Rad Laboratories, Hercules, CA,USA). Equal amounts of proteins were separated by 12.5% SDS-PAGE and electrotransferred by semidry blotting onto a nitrocellulose membrane. Membranes were incubated with rabbit anti-human polyclonal antibodies against MnSOD (Millipore, USA) and CuZnSOD (Millipore, USA). Blots were re-incubated with antibodies to actin (Millipore, USA) for protein loading correction. Immunoreactive polypeptide bands were visualized by using an enhanced chemiluminescence kit (Amersham, USA). Band intensities were quantitated by using AlphaImager 2000 (Alpha Innotech., San Leandro, CA, USA) and ImageJ software. The integrated density value was obtained by integrating the entire pixel values in the area of one band after correction for background. Fold change was calculated relative to control after correction for loading in individual samples.

2.5 Gel electrophoresis assay for measurements of MnSOD activity

Total cellular protein extracts were prepared by sonicating cells using a Vibra Cell Sonicator with cup attachment (Sonics and Materials Inc., Newtown, CT, USA). Equal amounts of proteins were separated by a 12.5% non-dissociating (native) PAGE following previously published methods (Beauchamp and Fridovich 1971; Sarsour et al. 2005; Sarsour et al. 2008). Gels were incubated with 2.43 mM nitroblue tetrazolum, riboflavin (2.8×10^{-5} M) and TEMED (28×10^{-3} M) for 20 min at room temperature. Gels were kept in distilled water and illuminated under bright fluorescent light until SOD bands were visualized. Sodium cyanide (0.75 mM) was used to distinguish between CuZnSOD and MnSOD activities. Quantitaion was performed by using AlphaImager 2000 (Alpha Innotech., San Leandro, CA, USA) and ImageJ software. Fold change was calculated relative to control.

2.6 Real Time PCR analysis

Total cellular RNA was isolated using the Trizol reagent (Invitrogen, Eugene,Oregon). RNA was quantified using a ND1000 nanodrop spectrophotometer (Nanodrop, Wilmington, Delaware) and one microgram of RNA from each sample was reverse transcribed using the High Capacity cDNA Archive Kit (Applied Biosystems, Foster city, California). The cDNA was subjected to Real Time PCR assay using primers specific to MnSOD open reading frame (ORF), and 18S as endogenous control; MnSOD, forward primer: 5'-GGCCTACGTGAACAACCTGAA-3', reverse primer: 5'-CTGTAACATCTCCCTTGGCCA-3' amplicon size, 70 bp. The real time PCR assay was done using 2× Power SYBR Green real time master-mix (Applied Biosystems); reverse transcriptase inactivation at 95°C for 10 min, followed by 40 cycles of 95°C for 15 sec and 60°C for 1 min (ABI 7000 Sequence Detection System, Applied Biosystems). A threshold of amplification in the linear range was selected to calculate the cycle threshold (C_T) for each sample. The relative mRNA levels were calculated as follows: ΔC_T (sample) = C_T (mRNA of interest) − C_T (18S); $\Delta\Delta C_T = \Delta C_T$ (post-treatment time point) − ΔC_T (control); Relative expression = $2^{-\Delta\Delta CT}$.

2.7 Electron spin resonance spectroscopy

Electron spin resonance (ESR) spectroscopy was performed using DMPO (5, 5-dimethyl-1-pyrroline N-oxide) as the spin trap, and Bruker EMX 300 spectrometer with a magnetic field modulation frequency of 100 KHz and microwave power of 40 mW. The scans were traced with modulation amplitude of 1 G and scan rate 80G/81s. Recorded Spectra were composed from an average of 15 scans. Monolayer cultures were washed with PBS and layered with 500 μL of PBS containing DMPO (100 mM) and chelated resin (iminodiacetic acid, sodium form, dry mesh 50–100; Sigma Chemicals). Cells were incubated for 15 min at 37°C, harvested by

scrapping, and transferred to a flat cell for ESR measurement. CuZnSOD (1000 units/ml) and Tiron (1 mM) were used to determine the specificity of the assay for the measurements of superoxide. ESR peak heights were measured using WinEPR software, and results were calculated relative to one million cells.

2.8 Assays for measurements of mitochondrial ROS and mass

Flow cytometry based measurements of MitoSOX and MitoTracker fluorescence were performed to determine mitochondrial ROS and mass following our previously published methods (Sarsour et al. 2008). Briefly, monolayer cultures were washed 3 times with warm Hanks buffer salt solution (HBSS), and incubated with 3 μM MitoSOX® and 0.5 μM MitoTracker Green® FM (Invitrogen) for 15 min. Cells were harvested by trypsinizing the monolayer cultures and resuspended in HBSS buffer containing 10% FBS. Flow cytometry measurements were performed using 488 nm excitation laser and 585/42 nm emission filter for MitoSOX, and 530/30 nm emission filter for MitoTracker fluorescence. Mean fluorescence intensity was analyzed using Flowjo software; autofluorescence of unlabeled cells was used for background correction.

2.9 Statistical analysis

Statistical analysis was done using the one and two-way analysis of variance with Tukey's honesty significant difference test. Homogeneity of variance was assumed with 95% confidence interval level. Results from at least $n \geq 3$ with $p < 0.05$ were considered significant. All statistical analysis were done using SPSS computer software Standard version 10.0.5 (SPSS Inc., Chicago, IL).

3. Results

3.1 Age associated mitochondrial abnormalities in quiescent fibroblasts

Previously, we have shown aged quiescent human normal skin fibroblasts (NHFs) were unable to reenter the proliferative cycle compared to young quiescent cultures (Sarsour et al. 2005). To determine if the inhibition in the proliferative capacity of aged quiescent fibroblasts was due to a loss in mitochondrial structural integrity, transmission electron microscopy was used to visualize mitochondrial morphology. Contact inhibited quiescent NHFs were cultured for 2–50 d in 21% oxygen environment and fresh medium was added every three days. Flow cytometry analysis of DNA content showed that more than 95% of the cells were in G_0/G_1 during the entire period of quiescence. Young quiescent cells, 2 days in quiescence, exhibited normal mitochondrial morphology with intact outer and inner membranes, and cristae (Figure 1A). However, a significant difference in mitochondrial morphology was observed in aged quiescent cultures, 50 days in quiescence. There were also irregularities in inner and outer membranes as well as significant loss in cristae (Figure 1A, lower panel).

MnSOD activity is known to protect quiescent NHFs from age associated loss in proliferative capacity (Sarsour et al. 2005). To determine if this protection is due to a prevention of mitochondrial morphology from age associated loss, transmission electron microscopy was used to visualize mitochondrial morphology in 50-day old control and MnSOD overexpressing cells. Quiescent NHFs were infected with 30 MOI of control (AdBgl II) and MnSOD (AdMnSOD) containing adenoviruses and continued in culture for 50 days. Results from immunoblotting and gel activity assays showed MnSOD overexpression increased MnSOD protein and activity by approximately 2 folds (Figure 1B). To determine if MnSOD overexpression alters cellular ROS levels, ESR measurements were performed in control and MnSOD overexpressing 50-day old quiescent cultures. Results showed significantly higher levels of ROS in control and AdBgl II infected cells (Figure 1C). MnSOD overexpressing quiescent cells exhibited significantly less cellular ROS levels compared to control and AdBgl

II infected cells. Interestingly, MnSOD activity induced suppression of ROS levels in aged quiescent NHFs was associated with protection of mitochondrial morphology (Figure 1A). These results support the hypothesis that age associated increase in cellular ROS levels damage mitochondrial morphology.

3.2 MnSOD activity and mitochondrial functions

A regulatory role of MnSOD activity and mitochondrial functions was further evident from results presented in Figure 2. MnSOD (+/+), heterozygous (+/−) and knock out (−/−) MEFs were cultured in a 4% oxygen environment and harvested for transmission electron microscopy analysis of mitochondrial morphology. Consistent with results presented in Figure 1A, MnSOD (+/+) MEFs showed normal mitochondrial morphology including elongated shapes with intact inner and outer membranes, and cristae (Figure 2A). In contrast, MnSOD (+/−) and MnSOD (−/−) MEFs showed varying levels of mitochondrial structural damage. MnSOD (+/−) MEFs have less cristae and more globular structures, while MnSOD (−/−) MEFs have a severe loss of the cristae and irregular membranes (Figure 2A). The changes in mitochondrial morphology were associated with a significant difference in mitochondrial functions. MitoTracker is a mitochondria specific dye that accumulates in active mitochondria and this accumulation is independent of the mitochondrial membrane potential (Presley et al. 2003). This property of the dye was used to measure the abundance of mitochondria in MnSOD genotype MEFs. Flow cytometry measurements of Mitotracker fluorescence showed highest levels of fluorescence in MnSOD (+/+) MEFs, while the fluorescence decreased 50% in MnSOD (−/−) MEFs (Figure 2B). A flow cytometry assay was used to measure mitochondrial ROS following our previously published method (Sarsour et al. 2008). MnSOD (−/−) MEFs exhibited highest MitoSOX fluorescence; MitoSOX fluorescence decreased 30% in MnSOD (+/−) and 60% in MnSOD (+/+) MEFs (Figure 2B). These results demonstrate an inverse correlation between MnSOD activity, and the abundance of mitochondria and mitochondrial ROS.

3.3 Oxygen environment and proliferative capacity of quiescent fibroblasts

An increase in cellular ROS levels combined with mitochondrial abnormalities and loss in the proliferative capacity of quiescent NHFs prompted us to determine if oxygen concentration influences these biological properties of quiescent NHFs. Quiescent NHFs were cultured for 60 days in 21% and 4% oxygen environments. Results from transmission electron microscopy showed significant damage to mitochondrial morphology in quiescent NHFs cultured in a 21% oxygen environment compared to a 4% oxygen environment (Figure 3A). NHFs cultured in a 21% oxygen environment showed dark vacuoles that were absent in cells cultured in a 4% oxygen environment. MnSOD protein levels increased significantly in NHFs cultured in 21 vs. 4 and 1% oxygen environment (Figure 3B upper panel), while there were no corresponding changes in MnSOD RNA levels (Figure 3B lower panel). The protein levels of CuZnSOD did not change among NHFs cultured in different oxygen environments. Changes in the mitochondrial generated ROS and subsequent changes in mitochondrial morphology accompany changes in the proliferative capacity of quiescent NHFs. This hypothesis is further supported by results presented in Figure 3C. NHFs cultured for 60 and 80 days in 21, 4, and 1% oxygen environments were replated at a lower cell density and cell numbers counted at the time of replating, and 2, 4, and 6 days post-replating. NHFs cultured in a 21% oxygen environment exhibited cell population doubling of 54 hours compared to 44 hours in cells cultured in a 4% oxygen environment (Figure 3C, left panel). NHFs cultured in a1% oxygen environment were still in the lag phase of growth until 4 days post-replating and a small increase in cell number was noticed at 6 days post-replating (Figure 3C, left panel). Eighty-day quiescent NHFs cultured in a 21% oxygen environment totally lost their proliferative capacity, while cells cultured in a 4% oxygen environment still exhibited significant proliferation following sub-culture (Figure 3C, right panel).

4. Discussion

Normal cells undergo a finite number of divisions prior to entering an irreversible growth state. This phenomenon of cellular aging is most commonly referred to as “Hayflick limit”, which is also known as replicative senescence or telomere theory of aging (Allsopp et al. 1992; Campisi 1996; Harley et al. 1992; Hayflick 1965; Hayflick 1975). Although the majority of aging research focuses on understanding the mechanisms regulating replicative senescence, there is a growing interest in understanding a separate type of cellular aging known as chronological life span. Chronological life span of cellular aging was originally described in yeast as the age associated loss in the capacity of quiescent (G_0) cells to reenter the proliferative cycle (Harris et al. 2003). We have reported previously a comparable phenomenon of chronological life span in quiescent normal human skin fibroblasts (Sarsour et al. 2005). In this previously published study, we have shown a significant inhibition in the percentage of S phase in cells replated from long duration quiescence compared to early quiescence. Interestingly, overexpression of MnSOD during quiescence facilitated entry into S phase in replated cells. These results were comparable to the proliferative capacity of cells in early quiescence, suggesting that MnSOD activity is involved in protecting cellular chronological life span. MnSOD is a nuclear encoded and mitochondrial matrix localized enzyme that converts mitochondrial generated superoxide to hydrogen peroxide. Therefore, MnSOD induced protection of chronological life span also suggests that mitochondrial functions and cellular ROS levels could significantly impact upon the proliferative capacity of quiescent normal human fibroblasts. A better understanding of the mechanisms regulating chronological life span is necessary because a majority of the proliferative competent cells *in vivo* resides in quiescent growth state.

The present study investigates the hypothesis that age associated increase in cellular ROS levels and abnormalities in mitochondrial morphology significantly inhibit the capacity of quiescent fibroblasts to reenter the proliferative cycle. Mitochondrial morphology was significantly impaired in old vs. young quiescent fibroblasts (Figure 1). The abnormalities in mitochondrial morphology in old quiescent fibroblasts were associated with an increase in cellular ROS levels, which correlated with a significant inhibition of cellular proliferation (Figure 3). MnSOD overexpression preserved mitochondrial morphology from age associated abnormalities and suppressed cellular ROS levels. MnSOD induced protection of mitochondrial morphology facilitated reentry of quiescent fibroblasts to the proliferative cycle following replating. The regulatory role of MnSOD activity in preserving mitochondrial morphology and suppressing age associated accumulation of cellular ROS was further evident from the results obtained from MnSOD genotype MEFs (Figure 2). MnSOD (−/−) MEFs appear to have a smaller number of mitochondria (or mitochondrial mass) compared to MnSOD (+/−) and (+/+) MEFs. It is not clear how lack of MnSOD activity could affect mitochondrial number or mass. One possible explanation could be that lack of MnSOD activity would increase mitochondrial ROS levels, which could damage mitochondria resulting in a subsequent loss in the number or mass of the mitochondria. Interestingly, MnSOD protein levels were significantly higher in cells cultured at 21 vs. 4% oxygen environment without a corresponding change in MnSOD mRNA levels (Figure 3B). These results suggest that a translational or post-translational mechanism regulates MnSOD protein levels in cells cultured at 21 vs. 4% oxygen environment. The role of mitochondrial generated ROS regulating cellular life span is also evident from a recent report by Schriner et al. (Schriner et al. 2005). The authors showed that mitochondrial specific expression of catalase extends the median and maximal lifespan of the transgenic mice over expressing mitochondrial catalase by 20%. This previously published report and results from our present study support the hypothesis that age associated accumulation of mitochondrial ROS negatively impacts upon cellular aging.

A regulatory role of mitochondrial ROS in cellular aging also suggests that oxygen environment could be a significant factor in regulating chronological life span. This notion is supported by results presented in Figure 3. Mitochondrial morphology was aberrant in quiescent NHFs cultured in a 21% oxygen environment compared to cells cultured in a 4% oxygen environment, suggesting that cellular ROS levels could be higher in cells cultured at 21 *vs.* 4% oxygen environment. An increase in cellular ROS levels was also accompanied with an increase in MnSOD protein levels in quiescent NHFs cultured in a 21% oxygen environment compared to cells cultured in 4 and 1% oxygen environments. Furthermore, quiescent NHFs cultured in a 21% oxygen environment significantly inhibited entry into the proliferation cycle, while cells cultured in a 4% oxygen environment retained their capacity to reenter the proliferation cycle.

These effects of oxygen concentration on cellular proliferative capacity are consistent with previous reports that show 21% oxygen represents an oxidative stress condition, which could be a critical determinant of cell's population doublings (PDs) (Packer and Fuehr 1977; Saito et al. 1995; Serrano and Blasco 2001; Wright and Shay 2002). An increase of 10–35% in PDs was observed for human lung fibroblasts WI-38 and IMR-90 cultured in a 10% oxygen environment compared to cells cultured in a 20% oxygen environment (Packer and Fuehr 1977). Furthermore, cellular senescence was expedited when IMR-90 cells cultured in a 1% oxygen environment were shifted to a 20% oxygen environment (Saito et al. 1995). Interestingly, IMR-90 cells transformed with SV40 large-T antigen did not exhibit any significant effects of oxygen tension on their PDs (Saito et al. 1995). Apparently oxygen sensitivity of PDs is lost during cellular transformation and the transformed cells were unable to exit the proliferative cycle. Our results showed that quiescent NHFs cultured in a 21% oxygen environment for a long duration suffer considerable mitochondrial structural damage and subsequently lost their capacity to reenter the proliferative cycle. These results suggest that MnSOD activity and mitochondrial function could regulate the proliferative capacity of quiescent fibroblasts. Our results are consistent with a previously published hypothesis of a "mitocheckpoint" contributing to the process of cellular aging through irreversible cell cycle arrest (Singh 2006).

In summary, our results show age associated abnormalities in mitochondrial morphology and cellular ROS levels significantly impacting upon the chronological life span of quiescent normal human skin fibroblasts.

Abbreviations

MnSOD	Manganese superoxide dismutase
ROS	Reactive oxygen species
NHFs	Normal human fibroblasts
CuZnSOD	Cupper zinc superoxide dismutase
EcSOD	Extra cellular superoxide dismutase
MEFs	Mouse embryonic fibroblasts
FBS	Fetal bovine serum
ESR	Electron spin resonance
MOI	Multiplicity of infection
PD	Population doubling

Acknowledgments

We thank, Mr. Jian Shao from the Central Microscopy facility for assisting with electron microscopy work, The University of Iowa ESR and Flow Cytometry cores for assisting with ESR spectroscopy and flow cytometry assays. Funding from McCord research foundation and NIH CA 111365 supported this work.

References

Allsopp RC, Vaziri H, et al. Telomere length predicts replicative capacity of human fibroblasts. Proc. Natl. Acad. Sci. U. S. A 1992;89:10114–10118. [PubMed: 1438199]

Asikainen TM, Huang TT, et al. Increased sensitivity of homozygous Sod2 mutant mice to oxygen toxicity. Free Radic. Biol. Med 2002;32:175–186. [PubMed: 11796207]

Balaban RS, Nemoto S, Finkel T. Mitochondria, oxidants, and aging. Cell 2005;120:483–495. [PubMed: 15734681]

Beauchamp C, Fridovich I. Superoxide dismutase: improved assays and an assay applicable to acrylamide gels. Anal. Biochem 1971;44:276–287. [PubMed: 4943714]

Borgstahl GE, Parge HE, et al. The structure of human mitochondrial manganese superoxide dismutase reveals a novel tetrameric interface of two 4-helix bundles.[erratum appears in Cell 1993 Feb 12;72 (3):following 476]. Cell 1992;71:107–118. [PubMed: 1394426]

Boveris A. Mitochondrial production of superoxide radical and hydrogen peroxide. Adv. Exp. Med. Biol 1977;78:67–82. [PubMed: 197811]

Campisi J. Replicative senescence: an old lives' tale? Cell 1996;84:497–500. [PubMed: 8598035]

Campisi J. Cancer, aging and cellular senescence. In Vivo 2000;14:183–188. [PubMed: 10757076]

Chance B. Electron transfer: pathways, mechanisms, and controls. Annu. Rev. Biochem 1977;46:967–980. [PubMed: 332068]

Chance B, Sies H, Boveris A. Hydroperoxide metabolism in mammalian organs. Physiol. Rev 1979;59:527–605. [PubMed: 37532]

Davidson BL, Allen ED, et al. A model system for in vivo gene transfer into the central nervous system using an adenoviral vector. Nat. Genet 1993;3:219–223. [PubMed: 8387378]

Finch CE. The biology of aging in model organisms. Alzheimer Dis. Assoc. Disord 2003;17:S39–S41. [PubMed: 12813205]

Finkel T, Holbrook NJ. Oxidants, oxidative stress and the biology of ageing. Nature 2000;408:239–247. [PubMed: 11089981]

Harley CB, Vaziri H, Counter CM, Allsopp RC. The telomere hypothesis of cellular aging. Exp. Gerontol 1992;27:375–382. [PubMed: 1459213]

Harman D. Aging: a theory based on free radical and radiation chemistry. J. Gerontol 1956;11:298–300. [PubMed: 13332224]

Harris N, Costa V, et al. Mnsod overexpression extends the yeast chronological (G(0)) life span but acts independently of Sir2p histone deacetylase to shorten the replicative life span of dividing cells. Free Radic. Biol. Med 2003;34:1599–1606. [PubMed: 12788479]

Hayflick L. The limited in vitro lifetime of human dipliod cell strains. Exp. Cell Res 1965;37:614–636. [PubMed: 14315085]

Hayflick L. Current theories of biological aging. Fed. Proc 1975;34:9–13. [PubMed: 1088947]

Hayflick L, Moorhead PS. The serial cultivation of human diploid cell strains. Exp. Cell Res 1961;25:585–621.

Li Y, Huang TT, et al. Dilated cardiomyopathy and neonatal lethality in mutant mice lacking manganese superoxide dismutase. Nat. Genet 1995;11:376–381. [PubMed: 7493016]

Liu R, Oberley TD, Oberley LW. Transfection and expression of MnSOD cDNA decreases tumor malignancy of human oral squamous carcinoma SCC-25 cells. Hum. Gene Ther 1997;8:585–595. [PubMed: 9095410]

Melov S, Doctrow SR, et al. Lifespan extension and rescue of spongiform encephalopathy in superoxide dismutase 2 nullizygous mice treated with superoxide dismutase-catalase mimetics. J. Neurosci 2001;21:8348–8353. [PubMed: 11606622]

Melov S, Schneider JA, et al. A novel neurological phenotype in mice lacking mitochondrial manganese superoxide dismutase. Nat. Genet 1998;18:159–163. [see comment]. [PubMed: 9462746]

Orr WC, Sohal RS. Extension of life-span by overexpression of superoxide dismutase and catalase in Drosophila melanogaster. Science 1994;263:1128–1130. [PubMed: 8108730]

Packer L, Fuehr K. Low oxygen concentration extends the lifespan of cultured human diploid cells. Nature 1977;267:423–425. [PubMed: 876356]

Perez VI, Van Remmen H, et al. The overexpression of major antioxidant enzymes does not extend the lifespan of mice. Aging Cell 2009;8:73–75. [PubMed: 19077044]

Presley AD, Fuller KM, Arriaga EA. MitoTracker Green labeling of mitochondrial proteins and their subsequent analysis by capillary electrophoresis with laser-induced fluorescence detection. J Chromatogr B Analyt Technol Biomed Life Sci 2003;793:141–150.

Saito H, Hammond AT, Moses RE. The effect of low oxygen tension on the in vitro-replicative life span of human diploid fibroblast cells and their transformed derivatives. Exp. Cell Res 1995;217:272–279. [PubMed: 7698226]

Sarsour EH, Agarwal M, et al. Manganese superoxide dismutase protects the proliferative capacity of confluent normal human fibroblasts. J. Biol. Chem 2005;280:18033–18041. [PubMed: 15743756]

Sarsour EH, Venkataraman S, et al. Manganese superoxide dismutase activity regulates transitions between quiescent and proliferative growth. Aging Cell 2008;7:405–417. [PubMed: 18331617]

Schriner SE, Linford NJ, et al. Extension of murine life span by overexpression of catalase targeted to mitochondria. Science 2005;308:1909–1911. [PubMed: 15879174]

Serrano M, Blasco MA. Putting the stress on senescence.[erratum appears in Curr Opin Cell Biol 2002 Feb;14(1):123]. Curr. Opin. Cell Biol 2001;13:748–753. [PubMed: 11698192]

Singh KK. Mitochondria damage checkpoint, aging, and cancer. Ann. N. Y. Acad. Sci 2006;1067:182–190. [PubMed: 16803984]

Smith JR, Pereira-Smith OM. Replicative senescence: implications for in vivo aging and tumor suppression. Science 1996;273:63–67. [see comment]. [PubMed: 8658197]

St-Pierre J, Buckingham JA, Roebuck SJ, Brand MD. Topology of superoxide production from different sites in the mitochondrial electron transport chain. J. Biol. Chem 2002;277:44784–44790. [PubMed: 12237311]

Staniek K, Nohl H. Are mitochondria a permanent source of reactive oxygen species? Biochim. Biophys. Acta 2000;1460:268–275. [PubMed: 11106768]

Wright WE, Shay JW. Historical claims and current interpretations of replicative aging. Nat. Biotechnol 2002;20:682–688. [see comment]. [PubMed: 12089552]

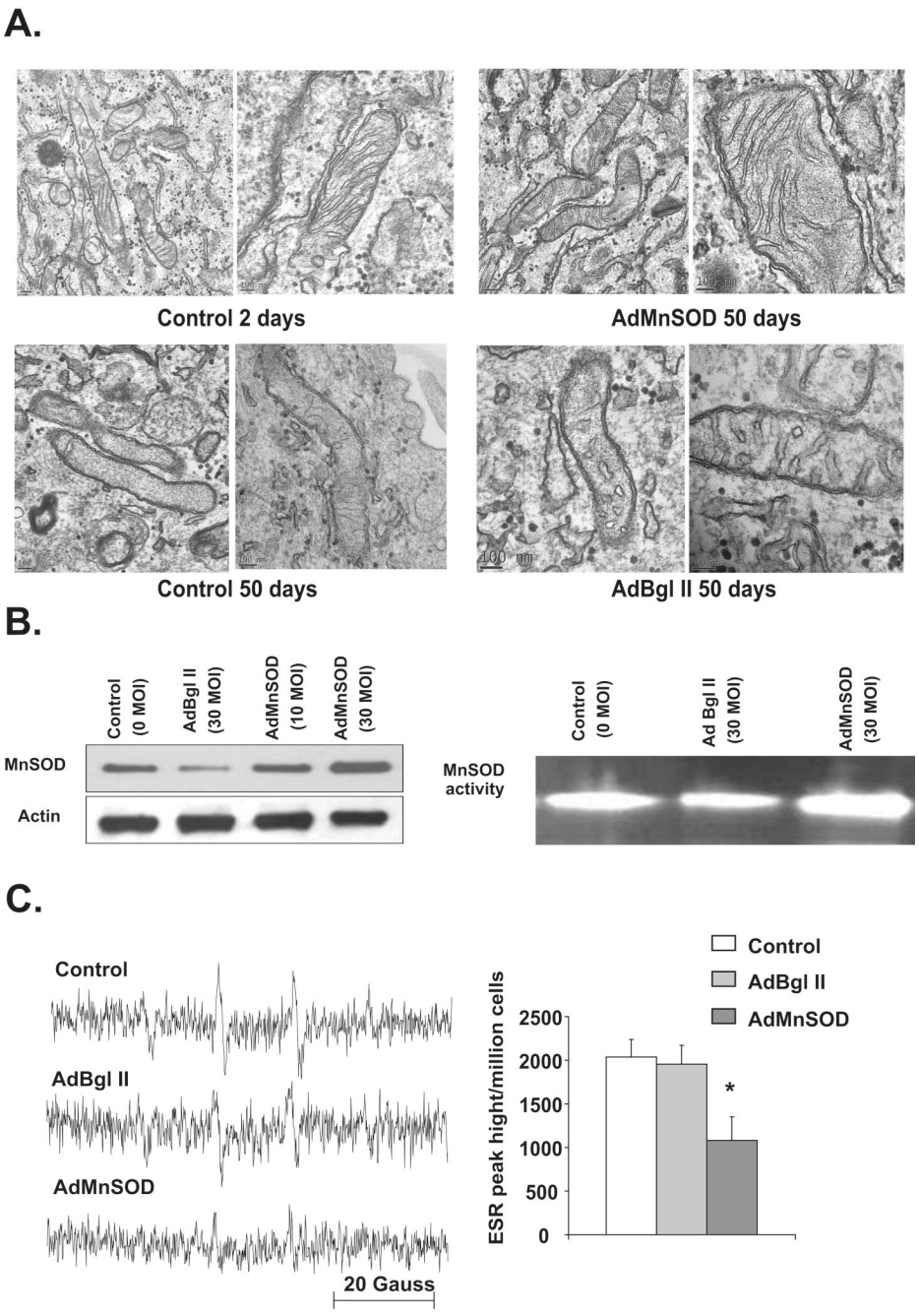

Figure 1. MnSOD overexpression protects mitochondrial morphology of quiescent NHFs from age associated abnormalities

A. Transmission electron microscopy pictures of mitochondria in young (2 days) and old (50 days) contact inhibited quiescent NHFs cultured in 21% oxygen environment (left panels). Two day old quiescent NHFs were infected with 30 MOI of AdBgl II and AdMnSOD adenoviruses, and cultured for a total of 50 days. Cells were collected by scraping and processed for visualization of mitochondrial morphology using transmission electron microscopy (right panels); scale ranges from 100 nm to 0.2 μm. Representative of 2 or more experiments. **B**. Total cellular protein extracts prepared from 7 days control and adenovirus infected quiescent NHFs were analyzed for MnSOD protein levels by immunoblotting (***Left panel***), and MnSOD

activity using native gel-electrophoresis assay (***Right panel***). **C**. Electron resonance spectroscopy measurements of cellular ROS levels in control, AdBgl II, and AdMnSOD infected quiescent NHFs; ***Left panel***: representative ESR spectra, ***Right panel***: ESR peak height per million cells. Asterisk indicates significant difference between MnSOD overexpressing NHFs compared to control, and AdBgl II infected cells. n=3, $p < 0.05$.

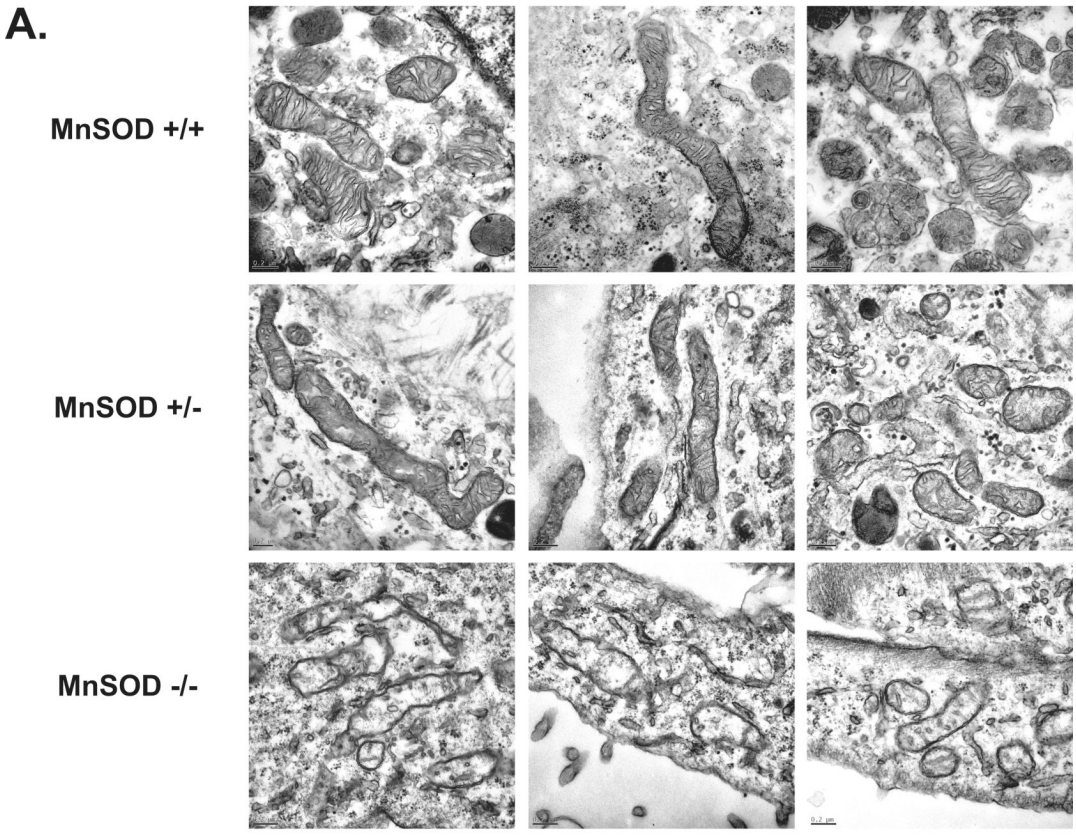

Figure 2. MnSOD activity protects mitochondrial morphology and suppresses cellular ROS levels

A. MnSOD genotype MEFs were cultured in 4% oxygen environment and harvested for transmission electron microscopy visualization of mitochondria morphology; scales range from 100 nm to 0.2 μm. Representative of 2 or more experiments. **B**. MnSOD genotype MEFs cultured in 4% oxygen environment were incubated with MitoTracker (**left panel**), and MitoSox (**right panel**). Fluorescence was measured by flow cytometry. Asterisks (left panel) indicate significant difference in MitoTracker fluorescence in MnSOD (−/−) compared to (+/+) and (+/−) MEFs; asterisks in right panel represent significant difference in MitoSOX fluorescence in MnSOD (+/+) and (+/−) compared to MnSOD (−/−) MEFs; n=3, $p<0.05$.

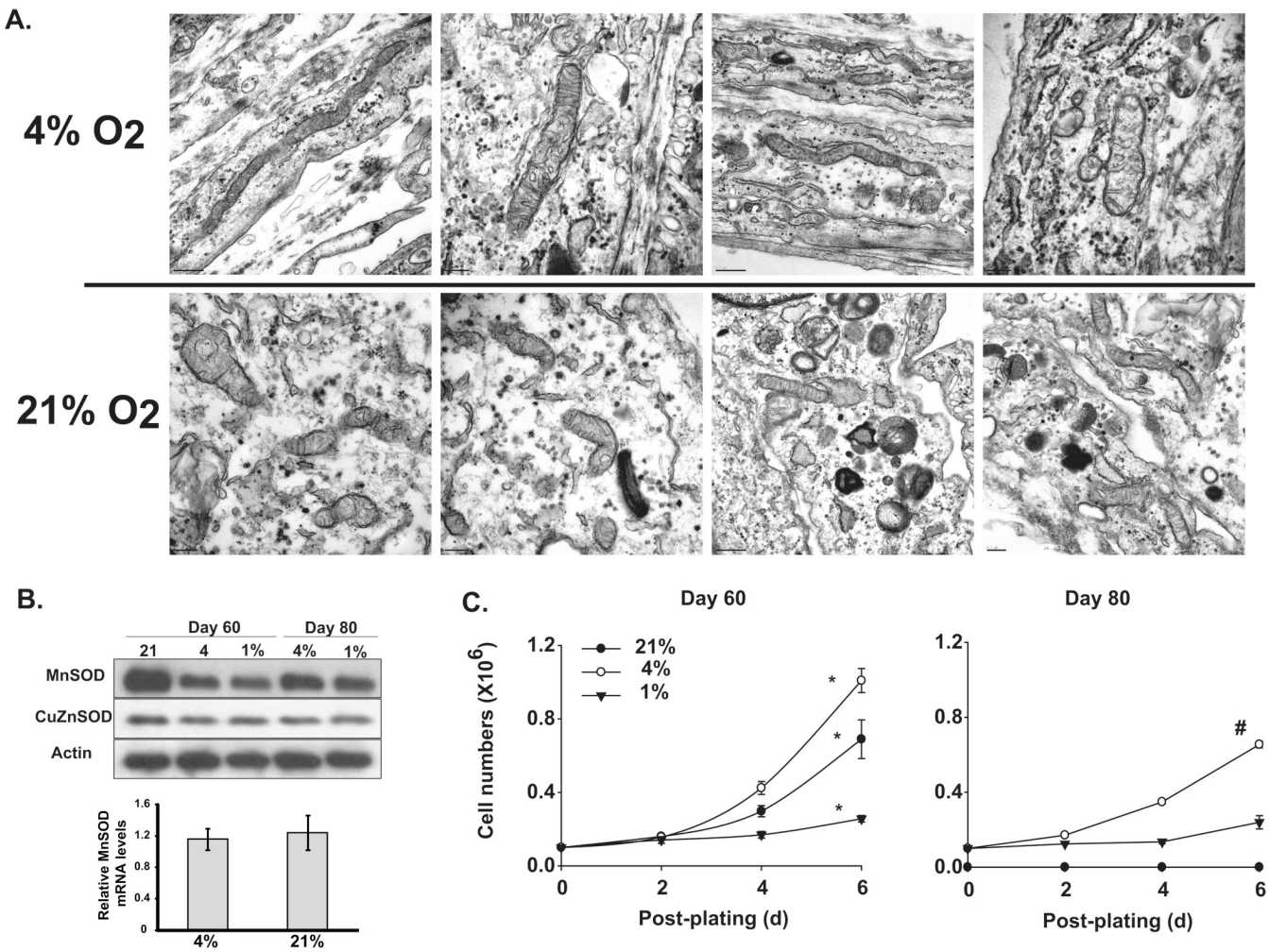

Figure 3. Lower oxygen environment protects quiescent NHFs from age associated abnormalities in mitochondrial morphology and loss in proliferative capacity

A. Transmission electron microscopy visualization of mitochondrial morphology in quiescent NHFs cultured in 1, 4, and 21% oxygen environment. Scales range from 100 nm to 0.2 μm. Representative of 2 or more experiments. **B. Upper panel**: total cellular protein extracts were analyzed for MnSOD and CuZnSOD protein levels by immunoblotting. Actin levels were used for loading correction. Quantitation was performed using Alpha Imager and Image J software. Band intensities were normalized to actin in individual samples and fold change calculated relative to control. **Lower panel**: Relative MnSOD mRNA levels in 12 days quiescent NHFs in 4% vs. 21% oxygen tension using real-time PCR as described in Materials and Methods. Relative MnSOD mRNA levels were calculated relative to 2-day quiescent NHFs. **C**. Growth characteristics of NHFs replated from 60 and 80 days quiescent NHFs cultured in 1, 4, and 21% oxygen environment. Replated cells were cultured in the same oxygen environment and cell numbers counted at indicated times. Asterisks indicate significant difference among different oxygen concentrations; # indicates significant difference in 80 days compared to 60 days quiescence; n=3, $p < 0.05$.